Acta Pharmaceutica Sinica B 2021;11(9):2945−2956

Chinese Pharmaceutical Association
Institute of Materia Medica, Chinese Academy of Medical Sciences

Acta Pharmaceutica Sinica B

www.elsevier.com/locate/apsb
www.sciencedirect.com

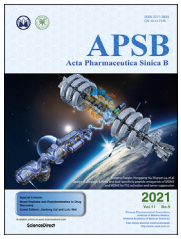

ORIGINAL ARTICLE

Reconstitution of biosynthetic pathway for mushroom-derived cyathane diterpenes in yeast and generation of new "non-natural" analogues

Ke Ma[a,b], Yuting Zhang[a,b], Cui Guo[a,b], Yanlong Yang[a], Junjie Han[a], Bo Yu[a,c], Wenbing Yin[a,b], Hongwei Liu[a,b,*]

[a]*State Key Laboratory of Mycology, Institute of Microbiology, Chinese Academy of Sciences, Beijing 100101, China*
[b]*Savaid Medical School, University of Chinese Academy of Sciences, Beijing 100049, China*
[c]*CAS Key Laboratory of Microbial Physiological and Metabolic Engineering, Institute of Microbiology, Chinese Academy of Sciences, Beijing 100101, China*

Received 28 February 2021; received in revised form 6 April 2021; accepted 12 April 2021

KEY WORDS

Cyathane-type diterpene;
Biosynthesis;
Heterologous expression;
Non-enzymatic reaction

Abstract Mushroom-derived cyathane-type diterpenes possess unusual chemical skeleton and diverse bioactivities. To efficiently supply bioactive cyathanes for deep studies and explore their structural diversity, *de novo* synthesis of cyathane diterpenes in a geranylgeranyl pyrophosphate engineered *Saccharomyces cerevisiae* is investigated. Aided by homologous analyses, one new unclustered FAD-dependent oxidase EriM accounting for the formation of allyl aldehyde and three new NADP(H)-dependent reductases in the biosynthesis of cyathanes are identified and elucidated. By combinatorial biosynthetic strategy, *S. cerevisiae* strains generating twenty-two cyathane-type diterpenes, including seven "unnatural" cyathane xylosides (**12**, **13**, **14a**, **14b**, **19**, **20**, and **22**) are established. Compounds **12**−**14**, **19**, and **20** show significant neurotrophic effects on PC12 cells in the dose of 6.3−25.0 μmol/L. These studies provide new insights into the divergent biosynthesis of mushroom-originated cyathanes and a straightforward approach to produce bioactive cyathane-type diterpenes.

*Corresponding author. Tel./fax: +86 10 64806074.
E-mail address: liuhw@im.ac.cn (Hongwei Liu).

Peer review under responsibility of Chinese Pharmaceutical Association and Institute of Materia Medica, Chinese Academy of Medical Sciences.

https://doi.org/10.1016/j.apsb.2021.04.014

1. Introduction

Cyathanes refer to a class of unique and mushroom-derived natural products possessing an angularly fused 5/6/7 tricyclic skeleton[1,2]. Basidiomycetes including *Hericium, Cyathus*, *Sarcodon*, *Phellodon*, *Strobilurus*, and *Laxitextum* species were reported to produce cyathane analogues with a broad spectrum of biological activities[3]. Erinacine A (**1**) possessing a rare cyclohepta-1,3-diene feature and notable potential to conquer neurodegenerative diseases was isolated from *Hericium erinaceus*[4,5]. Treatment with erinacine A exhibited beneficial effects on neurons, such as inhibiting the ROS-mediated neuron inflammation and death pathway[6], activating neuronal survival pathway[7], enhancing the synthesis of nerve growth factor[8], and promoting NGF-induced neurite outgrowth in nerve cells[9].

To ensure a sustainable supply of cyathanes for bioactivity investigation, chemists endeavoured to develop different total synthetic routes[10–12]. However, the currently reported approaches with harsh conditions and low yields were not amiable in industry. Recently, genetically engineered microbes had been successfully adopted for producing valuable natural products (such as opioids, artemisinic acid, and ganoderic acid)[13–15], which provides alternative strategy for the production of cyathanes. In our early work, we identified the gene cluster containing EriE (geranylgeranyl pyrophosphate synthase), EriG (UbiA-type terpene synthase), EriA/C/I (three P450 hydroxylases), and EriJ (glycosyltransferase) in *H. erinaceus* and characterized the function of EriG catalyzing the formation of the cyathane skeleton (Fig. 1)[16]. Genome mining among basidiomycetes revealed another three similar clusters with *eri*, including *rim* cluster from *Rickenella mellea*, *cya* cluster from *Cyathus striatus*, and *bom* cluster from *Bondarzewia mesenterica*. In the following work, Liu et al.[17] demonstrated the catalytic functions of *eriA*, *C*, *H*, *I*, and *J* together with an unclustered acetyl transferase EriL for the acetylation at 11-OH by heterologous expression in *Aspergillus oryzae* (Fig. 2). However, the production yields of cyathanes in *A. oryzae* is unsatisfactory. On the other hand, the gene responsible for the biosynthesis of α,β-unsaturated aldehyde group in cyathanes remains unknown. In the reported cyathanes, the α,β-unsaturated aldehyde group was not only the important structural feature of bioactive cyathane-type diterpenes, such as eriancine A (**1**), erinacine B (**2**), and erinacine P (**3**), but also accounted for the formation of C−C or C−O bond between xylose unit and cyathane aglycone as exemplified by striatoid C (**4**) and erinacine E (**5**) (Fig. 1A)[18–20].

In this study, we identified an unclustered FAD-dependent oxidase EriM responsible for the formation of allyl aldehyde in erinacines, demonstrated the allyl aldehyde-triggered nonenzymatic reactions in the biosynthesis of erinacines A–C. Furthermore, combinatorial biosynthetic routes leading to the *de novo* synthesis of 22 cyathanes were established in a geranylgeranyl pyrophosphate (GGPP)-engineered *Saccharomyces cerevisiae*.

2. Results

2.1. Divergent biosynthetic pathway for cyathanes derivatives

In the early report, heterologous expression of biosynthetic genes for erinacine Q (**6**) in *A. oryzae* generated a transformant strain with a low titer of 4.7 mg/L[17]. Thus, our first goal was to design an efficiency biocatalyst system to produce **6** with satisfactory yield in an engineered *S. cerevisiae* BY-T20, which had been engineered with high profit of GGPP[21]. The *eri* genes were introduced into δ sites or *rDNA* sites on the chromosome of *S. cerevisiae* with yeast promoters and terminators (Supporting Information Table S1) by homologous recombination. The cDNA of *eriG* was first integrated into yeast chromosome at the δ locus with P_{FBA1} promoter and T_{ADH1} terminator to give the transformant SC-G and

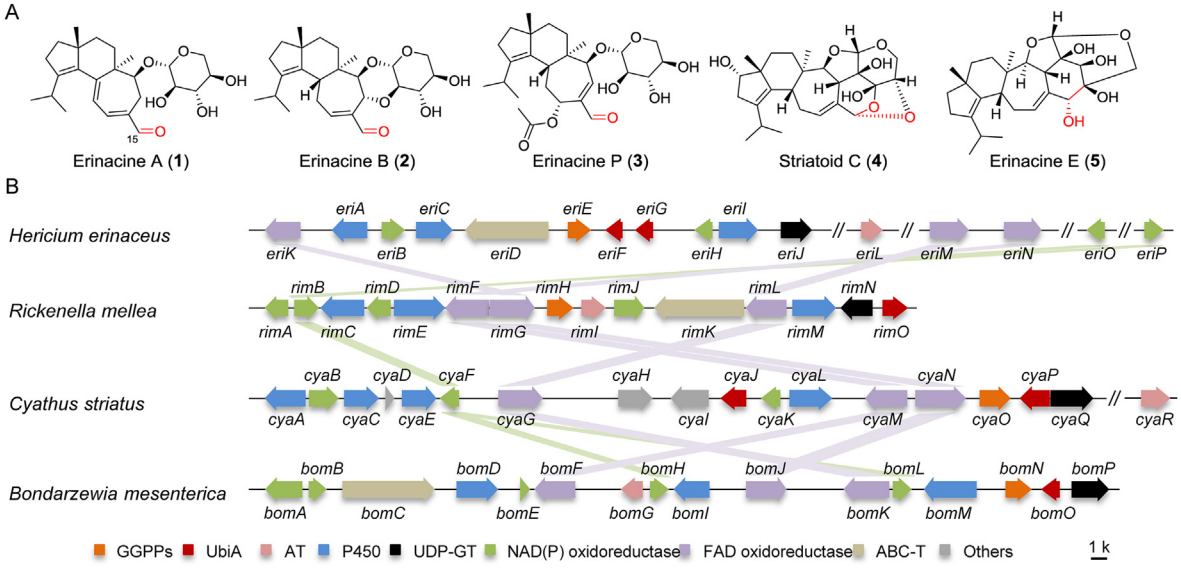

Figure 1 Representative structures of cyathanes (A), and the *eri* genes with their homologous (B).

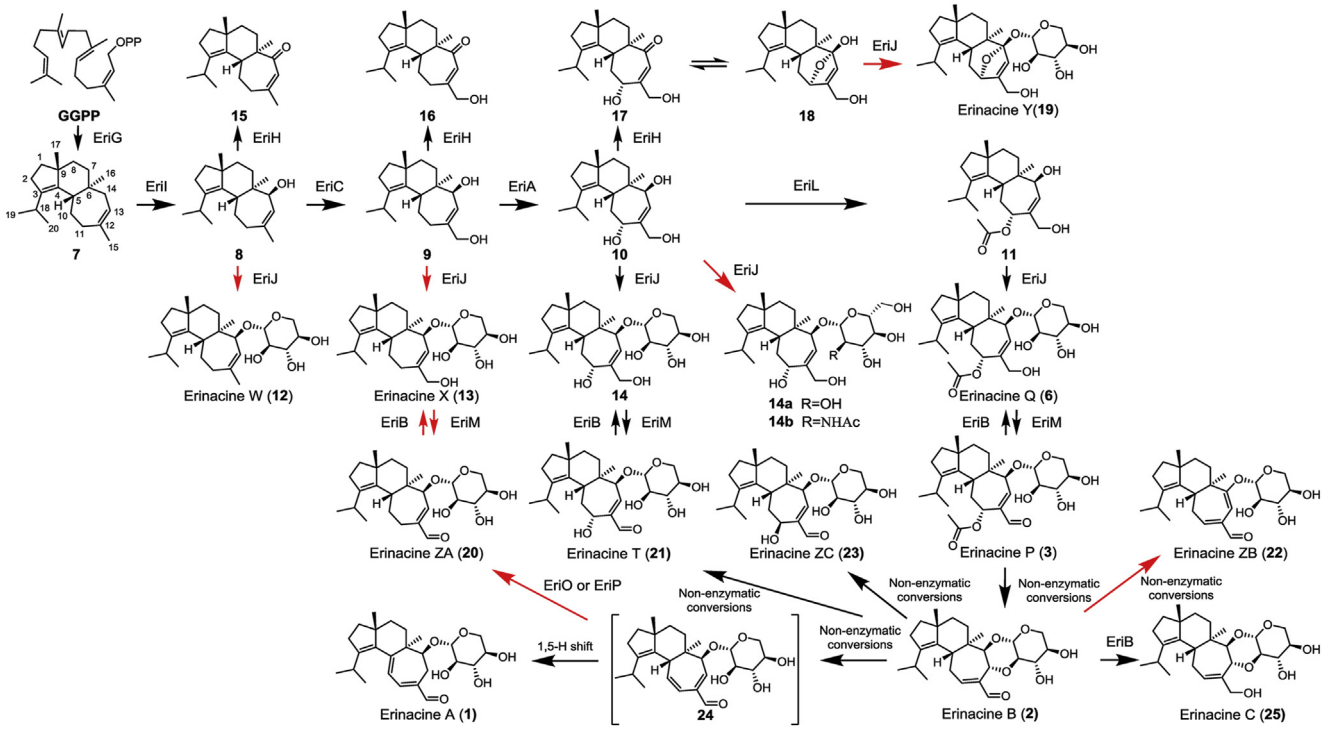

Figure 2 The modular biosynthetic pathway of erinacines. Arrows in red indicate the non-natural process in the formation of erinacines.

produce cyatha-3,12-diene (**7**) at a level of 105.8 mg/L (Fig. 3). Then, *ncpr1* (encoding for a NADPH-cytochrome P450 reductase in *S. cerevisiae*)[22], which was amplified from the genomic DNA of *S. cerevisiae* BY-T20, and *eriI* were co-expressed with *eriG* in the strain BY-T20. The resulting strain SC-GI produced a C-14 hydroxylated product (**8**, 79.3 mg/L). Similarly, transformants SC-GIC, SC-GICA, SC-GICAL, and SC-GICALJ were constructed. Genes *eriG*/*eriI*/*ncpr1* were integrated into δ sites, while genes *AtUGD1*[23], *AtUXS3*[23], and *eriJ/C/A/L* were introduced into *rDNA* sites of yeast chromosome. HPLC analysis of the broth extracts from these transformants showed the synthesis of **9–11** and erinacine Q (**6**) with the titers of 112.1, 88.5, 82.8, and 90.9 mg/L, respectively (Fig. 3 and Supporting Information Table S2).

In vitro enzymatic assays demonstrated that glycosyltransferase EriJ accepted **8**−**10** as substrates to catalyze the xylosylation of 14-OH and give the corresponding products **12**−**14** (Supporting Information Fig. S1). Thus, strains SC-GIJ, SC-GICJ, and SC-GICAJ were created and detected the synthesis of **12–14** with concentrations of 84.1, 100.3, and 98.4 mg/L (Fig. 3). In addition, the sugar nucleotide specificity test showed that EriJ could accept UDP-glucose and UDP-*N*-acetylglucosamine as donors, thus converting **10** into **14a** and **14b**, respectively (Supporting Information Fig. S2). Compounds **14a** and **14b** were successfully detected and isolated from the transformant SC-GICAJ (Supporting Information Tables S3 and S4).

Meanwhile, we generated transformants for the production of **15**, **16**, and cyathin A_3 (a mixture of **17** and **18**) by incorporating the EriH, a NAD/NADP-binding oxidase, into strains SC-GI, SC-GIC, and SC-GICA (Fig. 3). In the following, we transformed *eriH*-carrying plasmid into SC-GICAJ to generate a strain SC-GICAJH and obtained **19**. *In vitro* enzymatic assays also confirmed that EriH accepted **8**−**10** as substrates (Supporting Information Fig. S3). Erinacines W (**12**), X (**13**), and Y (**19**) are new unnatural caythane-xylosides. All compounds obtained from transformants were characterized by MS and NMR analyses (Tables 1 and 2)[24−28]. Collectively, these results strongly supported that divergent tailoring pathway in the biosynthesis of mushroom-originated cyathanes.

2.2. *Discovery of unclustered oxidoreductases in the genome of H. erinaceus*

After generating erinacine Q (**6**), **13**, and **14** in yeast, we proceeded to identify the enzyme responsible for aldehydation at C-15. Fungal FAD-dependent oxidoreductases were demonstrated to catalyze the formation of aldehyde in biosynthesis of solanapyrone A and glycine betaine[29,30]. Thus, we generated the transformant co-expressing *eriG/I/C/A/L/J* with the FAD-dependent oxidoreductase encoded gene *eriK*. The obtained strain SC-GICALJK failed to synthesis erinacine P (**3**) (Supporting Information Fig. S4), thus suggesting a potential unclustered gene for such reaction.

Next, we searched for FAD-dependent oxidoreductase genes in the *rim* cluster from *R. mellea*, *cya* cluster from *C. striatus*, and *bom* cluster from *B. mesenterica*. Cyathane-type diterpenes have been reported from the mushroom *C. striatus*[31]. As a result, two conservative FAD-dependent oxidase genes in the *rim* (*rimF* and *rimL*), *cya* (*cyaG* and *cyaM*), and *bom* (*bomF* and *bomK*) cluster,

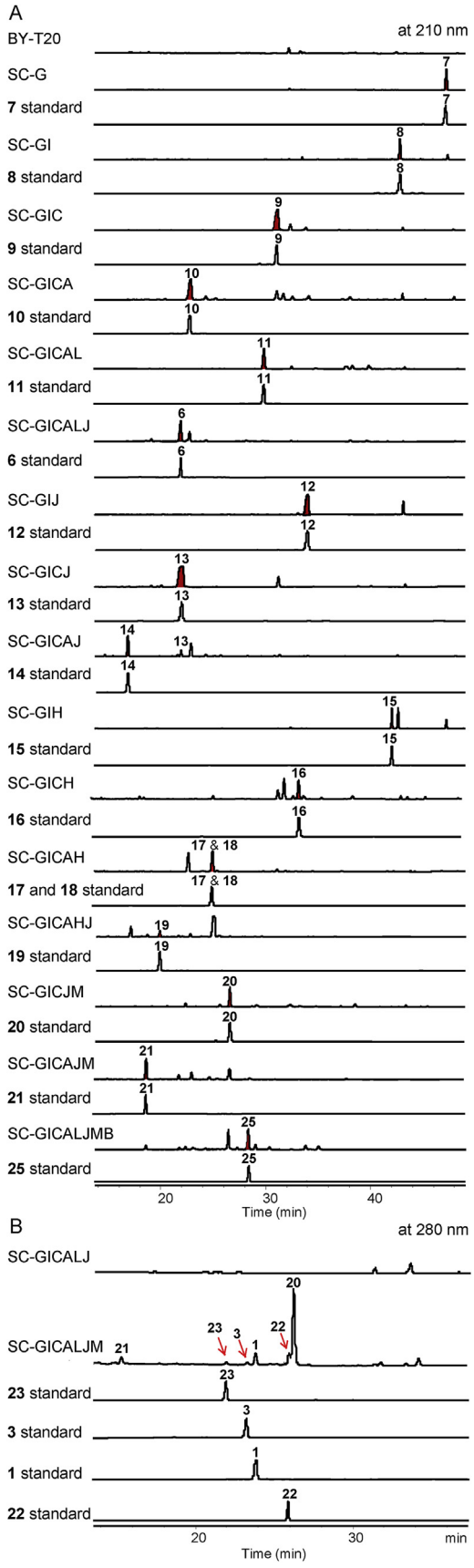

Figure 3 HPLC analyses of transformants expressing different biosynthetic enzymes.

were discovered, respectively (Fig. 1B and Supporting Information Table S5). With RimF and RimL as query sequences, two homologous proteins EriM with 65.6% dentity of RimL and EriN with 67.8% identity of RimF were identified from *H. erinaceus*. Similarly, additional two unclustered NAD(P)/NAD(P)H oxidoreductases (EriO and EriP) with 55%−78% sequence identities of RimB, CyaF, BomH, and BomL were also found in the genome of *H. erinaceus* (Fig. 1B and Table S5).

2.3. *Identification of catalytic functions of EriM and EriN*

To determine the functions of *eriM* and *eriN*, transformants SC-GICJM, SC-GICJN, SC-GICAJM, SC-GICAJN, SC-GICALJM, and SC-GICALJN were constructed. HPLC analyses showed the synthesis of metabolites **20** and erinacine T (**21**) and the formation of erinacine P (**3**) in the strains SC-GICJM, SC-GICAJM, and SC-GICALJM, respectively (Fig. 3). Compound **20** was a new cyathane-type diterpene whose structure was determined by HR–MS and NMR data analysis. Accordingly, the function of EriM was deduced to catalyze the oxidation of the allyl alcohol. To further verify the catalytic function of EriM, substrates **6**, **13**, and **14** were fed to the transformant SC-M bearing expression plasmid of pESC-TRP-EriM, respectively. As a result, the corresponding oxidation products **3**, **15**, and **16** (Fig. 4) were obtained, which definitely confirmed the oxidizing function of EriM on allyl alcohol (Fig. 2). However, no products were detected in the culture of the transformant SC-M when fed with different substrates **9**, **10**, **11**, **16** and **17**.

2.4. *Revealing non-enzymatic spontaneous reaction in the formation of erinacines A (**1**), B (**2**), T (**21**), and ZC (**23**)*

To our surprise, besides **3**, the transformant SC-GICAJLM produced another three metabolites **1**, **22**, and **23**. After a large scale fermentation of SC-GICAJLM, we successfully obtained compounds **1** (30.5 mg), **22** (5.8 mg), and **23** (2.5 mg). Further HRTOF-MS and NMR analyses assigned **1** to be erinacine A[4]. The HRTOF-MS and 1D NMR data of **22** indicated a similar structure with that of **1**. The main differences between **1** and **22** lie in the chemical shifts of olefinic protons (δ_H 6.79, d, J = 8.0 Hz and 5.78, d, J = 8.0 Hz in **1**; δ_H 6.88, t, J = 6.0 Hz and 5.81, s in **22**) (Table 2). The HMBC correlations from H-11 (δ_H 6.88) to C-5/C-10/C-13/C-15 and H-13 to C-6/C-11/C-12/C-14/C-15 determined the cyclohepta-1,6-diene-1-carbaldehyde moiety in **22** (Fig. 2). Compound **23** was identified to be an epimer of **21** by 2D NMR data analysis (Table 2). The HMBC correlations from H-11 to C-5/C-10/C-12/C-13/C-15 and NOE correlations from H-11 to H-14 confirmed a β-hydroxyl group at C-11 in **23**.

Kenmoku et al.[18] reported the chemical transformation of **3** to **1** *via* **2** by sequential Michael addition−elimination, which in combination with the co-existence **1** and **3** in the transformant SC-GICAJLM proposed the non-enzyme reaction in the formation of **1**. To test our hypothesis, strains SC-M and BY-T20 were fed with **3**, respectively. HPLC analysis of broth extracts showed the conversion of **3** to **1** (yield 29%), **21** (yield 4%), and **22** (yield 2%) (Supporting Information Fig. S5), supporting the occurrence of spontaneous reactions. Further *in vitro* incubation of **3** in buffer solution (pH = 7.5, the pH value at endpoint of fermentation) at 28 °C resulted in the formation of **1**, **2**, and **21** (Supporting Information Fig. S6). Additionally, it was found that high temperature and high pH facilitated the formation of **2** and the

Table 1 ^{1}H and ^{13}C NMR data of **12**, **13**, and **19** in 500 MHz.

12[a]			**13**			**19**		
No.	δ_C	δ_H mult. (*J* in Hz)	No.	δ_C	δ_H mult. (*J* in Hz)	No.	δ_C	δ_H mult. (*J* in Hz)
1	39.2	1.58, m 1.51, (overlapped)	1	37.7	1.51, m 1.46 (overlapped)	1	39.0	1.48 (overlapped) 1.40 (overlapped)
2	29.3	2.30 (overlapped)	2	27.8	2.22, t (7.6)	2	26.2	1.22 (overlapped) 1.40 (overlapped)
3	140.0	–	3	139.7	–	3	138.2	–
4	141.3	–	4	138.0	–	4	136.7	–
5	44.6	2.94, d (11.8)	5	43.1	2.88, d (11.4)	5	41.3	2.34, d (11.0)
6	44.6	–	6	42.8	–	6	47.7	–
7	34.2	2.21 (overlapped) 1.14 (overlapped)	7	32.6	1.02 (overlapped) 2.19 (overlapped)	7	29.6	2.19 (overlapped)
8	38.1	1.51 (overlapped) 1.41, ddd (12.9, 4.7, 2.6)	8	36.8	1.41 (overlapped) 1.33, m	8	36.9	1.61 (overlapped) 1.36, m
9	50.5	–	9	49.1	–	9	47.7	–
10	27.2	1.92 (overlapped) 1.08, m	10	26.0	1.80, m 1.71, m	10	28.4	2.03, t (12.7) 1.48 (overlapped)
11	33.9	2.57, dd (14.6, 10.8) 1.98 (overlapped)	11	28.1	2.37, m 1.87 (overlapped)	11	77.5	4.64, br
12	142.1	–	12	143.7	–	12	148.7	–
13	125.6	5.52, d (6.9)	13	123.1	5.60, d (6.8)	13	123.2	5.99, s
14	87.7	3.59, d (6.9)	14	84.6	3.56, d (6.8)	14	112.8	–
15	26.0	1.74, s	15	65.3	3.76, d (5.0)	15	57.0	4.08 (overlapped)
16	17.4	0.83, s	16	16.4	0.73, s	16	11.9	0.91, s
17	25.0	1.10, s	17	24.5	1.04, s	17	24.0	0.91, s
18	28.1	3.06, dd (6.8)	18	26.3	2.98 (overlapped)	18	25.7	2.91 (overlapped)
19	22.0	0.98, dd (11.2, 6.8)	19	21.9	0.92, d (6.7)	19	22.4	0.97, d (6.7)
20	22.3	0.98, dd (11.2, 6.8)	20	21.6	0.91, d (6.7)	20	21.1	0.87, d (6.7)
1′	107.0	4.27, d (7.0)	15-OH	–	4.73, t (5.5)	15-OH	–	4.98, t (5.4)
2′	75.3	3.26, dd (8.8, 7.0)	1′	105.8	4.13, d (7.3)	1′	97.2	4.43, d (7.4)
3′	77.7	3.32 (overlapped)	2′	73.8	3.02 (overlapped)	2′	73.0	2.98 (overlapped)
4′	71.2	3.48, ddd (9.6, 8.3, 5.1)	2′-OH	–	4.95, d (5.5)	2′-OH	–	4.50, d (5.0)
5′	66.6	3.83, dd (11.5, 5.1) 3,16, dd (11.6, 9.6)	3′	76.5	3.10, m	3′	76.3	3.09, m
			3′-OH	–	4.87, d (4.6)	3′-OH	–	4.91, d (4.7)
			4′	69.5	3.26, m	4′	69.4	3.27, m
			4′-OH	–	4.90, d (5.0)	4′-OH	–	4.91, d (4.7)
			5′	65.5	2.98 (overlapped) 3.62, dd (11.3, 5.2)	5′	65.4	2.94 (overlapped) 3.68, dd (11.3, 5.2)

[a]**12** was tested in methanol-d_4, **13** and **19** were tested in DMSO-d_6.

Table 2 ^{1}H and ^{13}C NMR data of **20**, **22**, and **23** (DMSO-d_6, 500 MHz).

20			**22**			**23**		
No.	δ_C	δ_H mult. (*J* in Hz)	No.	δ_C	δ_H mult. (*J* in Hz)	No.	δ_C	δ_H mult. (*J* in Hz)
1	37.5	1.51 (overlapped) 1.47 (overlapped)	1	36.5	1.55 (overlapped) 1.50 (overlapped)	1	37.3	1.47 (overlapped)
2	28.1	2.23, t (7.6)	2	27.9	2.27, t (7.1)	2	28.3	2.25, t (7.8)
3	138.9	–	3	139.6	–	3	138.5	–
4	138.7	–	4	137.7	–	4	139.0	–
5	42.4	2.87, br	5	42.4	2.54, t (6.0)	5	35.1	3.28 (overlapped)
6	43.0	–	6	48.3	–	6	43.6	–
7	32.2	1.18, m 2.15, m	7	33.6	1.63, td (13.8, 4.0) 1.77, dt (13.8, 4.0)	7	32.3	1.46 (overlapped) 1.14, br
8	25.0	1.45 (overlapped) 1.35, m	8	34.8	1.41, td (12.7, 4.0) 1.26, dt (12.7, 4.0)	8	36.2	1.51 (overlapped) 1.37, dt (12.3, 3.5)
9	49.0	–	9	49.5	–	9	49.3	–
10	25.0	1.78 (overlapped) 1.72 (overlapped)	10	30.2	2.78, t (6.0)	10	33.5	1.98, m
11	21.8	2.35, m 2.50 (overlapped)	11	151.7	6.88, t (6.0)	11	61.3	4.63, br
12	144.1	–	12	136.4	–	12	145.9	–
13	154.2	6.88, d (6.6)	13	92.4	5.81, s	13	153.8	6.95, d (7.0)
14	83.9	3.91, d (6.6)	14	168.6	–	14	83.3	3.93, d (7.0)
15	194.2	9.39, s	15	193.4	9.27, s	15	194.1	9.38, s
16	15.9	0.76, s	16	18.5	1.11, s	16	15.6	0.72, s
17	24.4	1.04, s	17	23.9	0.95, s	17	24.3	1.08, s
18	26.4	2.92 (overlapped)	18	26.6	2.92, m	18	26.4	2.95, m
19	21.6	0.91, d (6.7)	19	21.9	1.01, d (6.7)	19	21.9	0.93, d (7.2)
20	21.6	0.90, d (6.7)	20	21.2	0.97, d (6.7)	20	21.6	0.92, d (7.2)
1′	105.8	4.19, d (7.3)	1′	101.0	4.51, d (6.8)	1′	105.4	4.32, d (6.6)
2′	73.5	3.04 (overlapped)	2′	72.9	3.15 (overlapped)	2′	73.0	3.06 (overlapped)
2′-OH	–	5.08, d (5.6)	3′	76.3	3.17 (overlapped)	3′	75.0	3.17, m
3′	76.4	3.12, m	4′	69.3	3.34, m	4′	69.2	3.28 (overlapped)
3′-OH	–	4.91, d (4.9)	5′	65.5	3.13 (overlapped) 3.77, dd (11.3, 5.2)	5′	65.0	3.68, dd (11.5, 4.7) 3.09 (overlapped)
4′	69.5	3.26, m						
4′-OH	–	4.92, d (5.2)						
5′	65.6	3.02 (overlapped) 3.62, dd (11.3, 5.2)						

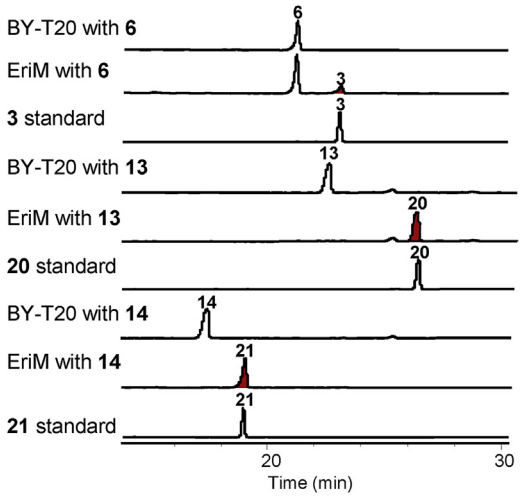

Figure 4 Feeding experiments of EriM with substrates **6**, **13**, and **14** by using BY-T20 as a control strain. Compounds were detected at 210 nm.

transformation from **2** to **1** and **21** (Supporting Information Fig. S7). Compound **2** was produced in advance of **1** in the solution. Thus, **2** was purified from the mixture of **3** incubated in an optimized condition. Furthermore, compound **2** was found to be converted into **1**, **21**, and **23** under the same condition (Supporting Information Fig. S8). These results demonstrated the FAD oxidase-driven and spontaneous Michael addition−elimination reactions in the biosynthesis of erinacines A (**1**), B (**2**), T (**21**), and ZC (**23**) from erinacine P (**3**) (Scheme 1). The formation mechanism of **22** in both strains SC-M and BY-T20 deserves further study.

2.5. *Generation of erinacine C and functions of EriP and EriO*

Next, to corroborate the functions of three unsolved NAD(P)/NAD(P)H oxidoreductases EriB, EriO, and EriP, strains SC-B, SC-O, and SC-P were created by introducing the plasmids pESC-TRP-EriB, pESC-TRP-EriO, and pESC-TRP-EriP into BY-T20, respectively. Feeding experiments with **3** revealed that strain SC-B transformed **3** into **6** and **25** (Fig. 5) that was determined to be erinacine C by NMR data comparison with the published values[4]. Next, the engineered stain SC-GICALJMB expressing *eriG/I/C/A/L/J/M/B* produced **25** with a yield of 43.6 mg/L (Fig. 3A). Our attempt to purify EriB in yeast was unsuccessful. To definitely confirm the function of EriB, microsome of EriB was prepared by the reported method[32]. Incubation of EriB microsome with **2**, **3**, **20**, and **21** in the presence of NADPH generated the corresponding reducing products **25**, **6**, **13**, and **14**, respectively (Fig. 5C). Based on these results, EriB was defined as an NADPH reductase catalyzing the reduction of allyl aldehyde. For the strains of SC-O and SC-P, feeding experiments with **3** gave the same metabolite **20** (Fig. 5). Purification of EriP in yeast was successful while the attempt to purify EriO was failed. Further *in vitro* enzymatic reactions using purified EriP with **2** or **3** as substrate gave the same product **20** in the presence of NADP (Fig. 5B).

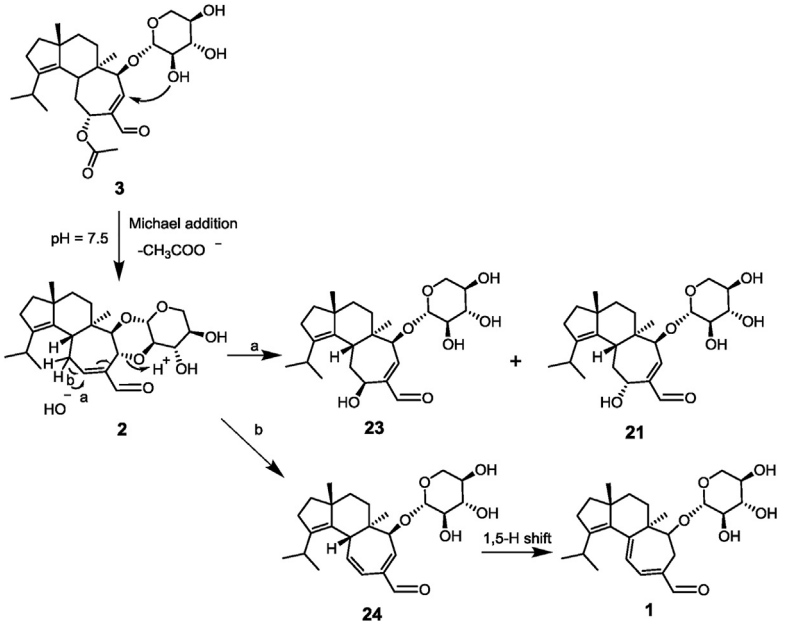

Scheme 1 Mechanisms for spontaneous synthesis of **1**, **21**, and **23** from **3** *via* **2**.

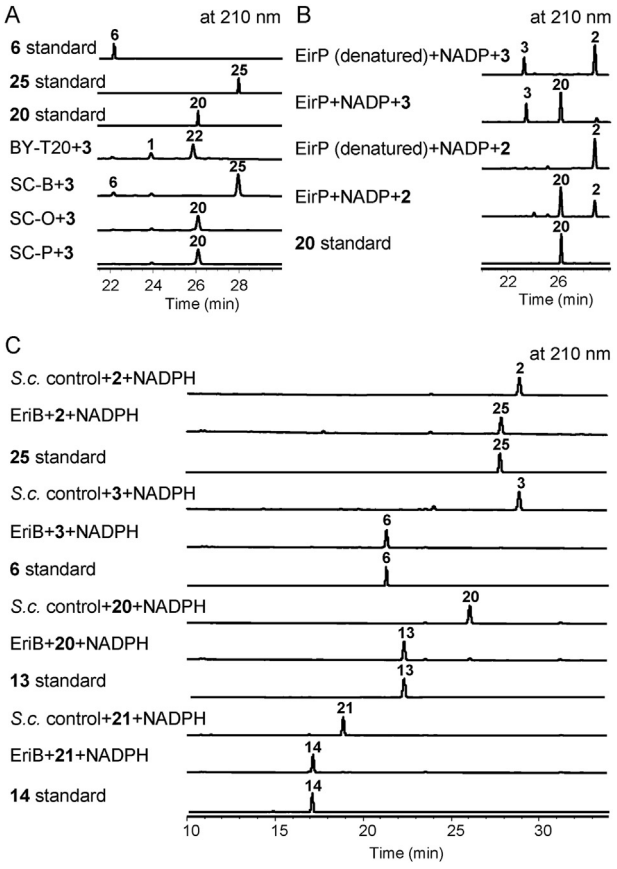

Figure 5 HPLC analysis for products of EriB, EriO, and EriP. (A) Feeding experiments of SC-B, SC-O, and SC-P with **3**. (B), *In vitro* enzymatic reactions of EriP with **2** and **3**. (C), *In vitro* assay of EriB (microsome) with **2**, **3**, **20**, and **21** as substrates.

Postulating **24** as the key intermediate for the spontaneous transformation from **2** or **3** to **1**, we supposed it as the true substrate of EriO and EriP.

2.6. *Neurite-promoting activities of new cyathane xylosides*

Mushroom-derived cyathane diterpenes were demonstrated to be promising leads with potent neuroprotective and neurotrophic activities[28,33,34]. In the course of our work, four new cyathane xylosides (**12**, **13**, **19**, and **20**) and one intermediate **14** were obtained at a level of 84.1, 100.3, 17.2, 92.5, and 98.4 mg/L, respectively. We tested their neurite-promoting activities by using PC12 cell line. The effects of compounds **12**−**14**, **19**, and **20** on the neurite outgrowth of undifferentiated PC12 cells were evaluated by morphological observations and a quantitative analysis of neurite-bearing cells. All these five compounds showed significant neurotrophic effects in the range of 6.3−25.0 μmol/L, as compared with the group that used NGF with neurite-bearing cells of 11.5 ± 1.3% at the concentration of 2.0 ng/mL (Fig. 6). The preliminary structure−activity relationship analysis shows that hydroxylation at C-11 and C-15 benefits for the neurotrophic effects, which was indicated by the higher activity of **13** and **14** than that of **12**. All above evidences provided new evidence supporting the combinatorial biosynthetic strategy as an effective way to expand the chemical space of bioactive natural products.

3. Discussion

Numerous natural products with attractive bioactivities have been characterized from cultures or fruiting bodies of mushroom[35−38]. More importantly, some of mushroom-derived bioactive compounds are being under clinical investigations. Lefamulin, a derivative of pleuromutilin (one diterpene isolated from *Clitopilus passeckerianus*), has been approved for the treatment of community-acquired pneumonia in 2019[39]. Irofulven, an analog of illudin S (one sesquiterpene from *Omphalotus olearius*), exhibites activities in shrinking malignant solid tumors and drug-resistant cancers during phase I clinical trials[40]. As to mushroom-derived cyathane derivatives, an erinacine A-enriched mycelia extract of *H. erinaceus* have showed an improvement in cognitive functions in 50- to 80-year-old Japanese men and women diagnosed with mild cognitive impairment[41]. However, the difficulty in preparing erinacines from *H. erinaceus* limits further human pilot studies[42].

With the advance of synthetic biology tools and methods, microbes including *Escherichia coli*, *S. cerevisiae*, *Aspergillus nidulans*, and *A. oryzae* have been developed as efficient heterologous hosts for the generation of valuable natural products from plants and mushrooms[43−45]. For example, artemisinic acid, a precursor of artemisinin, is produced in an engineered *S. cerevisiae* by expression a plant dehydrogenase and a second cytochrome, with the titer of 25 g/L[46]. Opioids are completely biosynthesized in yeast by expression of 23 enzymes from plants, mammals, bacteria and yeast[13]. Tropane alkaloids are produced in an engineered baker's yeast by expression more than 20 proteins from microbes, plants and animals across six sub-cellular locations of cytosol, mitochondrion, chloroplast, peroxisome, ER membrane and vacuole[47].

Diterpens are synthesized from GGPP which is derived from the mevalonate pathway or the methylerythritol phosphate pathway. Thus, the GGPP-engineered *S. cerevisiae* strains including BYT20 used in this work have potential to address challenges facing in the production of bioactive diterpenes. Recently, the plant-derived miltiradiene (the precursor of tanshinone), levopimaric acid, and sclareol have been successfully synthesized in the *S. cerevisiae* strains engineered with high profits of GGPP and their production yields are further improved by comprehensive engineering approaches[48−51].

In this work, we achieved *de novo* biosynthesis of 22 cyathane diterpenes including erinacines A–C, P, and T in the *S. cerevisiae* BYT20, and identified an unclustered EriM-coded FAD-dependent oxidase for aldehyde modification of erinacines in the genome of *H. erinaceus*. The formation of allyl aldehyde is critical for the structural variability in the cyathanes family and their potent anticancer activity and beneficial effects on neurons[3,34]. The spontaneous nonenzymatic reactions including the tandem Michael addition−elimination were demonstrated in the formation of erinacines A–C. In addition, a new NADPH reductase EriB catalyzing the reduction of allyl aldehyde was identified and characterized. Furthermore, based on the substrate flexibility of EriJ, EriM, and EriH, we generated the GGPP-engineered *S. cerevisiae* producing seven "non-natural" cyathane xylosides (**12**, **13**, **14a**, **14b**, **19**, **20**, and **22**) by combinatorial biosynthetic strategy. Compounds **12**, **13**, **19**, and **20** were attested to enhance the neurite outgrowth of undifferentiated PC12 cells *in vitro*. The yields of 13 known cyathane diterpenes including erinacines A, C, Q, and T and 4 "unnatural" analogues (**12**, **13**, **19**, and **20**) in the GGPP-engineered *S. cerevisiae* reaches in the range of 13.4−112.1 mg/L (Table S2).

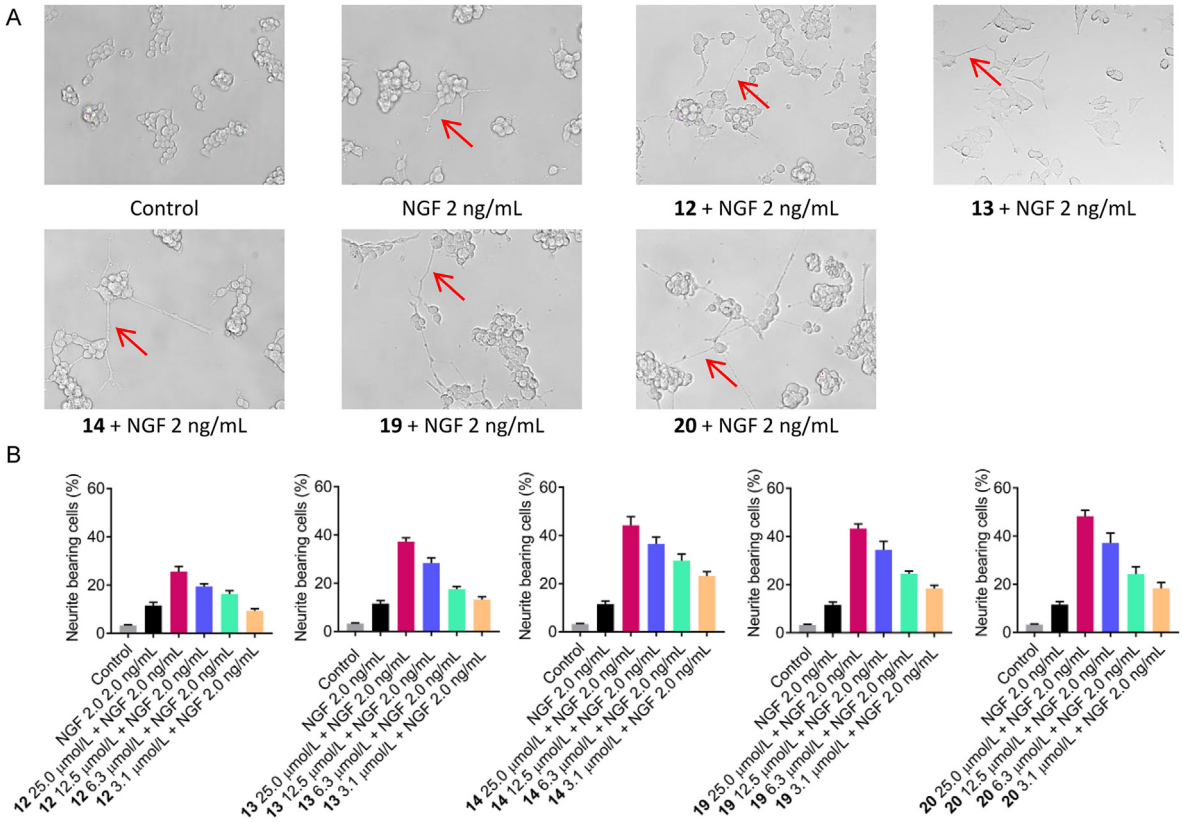

Figure 6 Neurite outgrowth of PC12 cells after 24 h treatment with NGF and compounds. (A), Neurites of PC-12 cells treated with NGF (2.0 ng/mL) or compounds (25 μmol/L). (B), The percentage of positive neurite-bearing cells treated with NGF and compounds. All plots show mean ± SD for $n = 3$ replicates.

Further studies are needed to elevate the production level of target compound. The substrate flexibility of EriB, EriJ, EriM, and EriH contributes to the structural diversity in the family of cyathanes. Discovery of *eri*-like gene clusters in the genome of *R. mellea* and *B. mesenterica* reveals their potential in producing cyathane derivatives.

4. Conclusions

This study gives insights into the biosynthesis of cyathanes, provides *S. cerevisiae* strains producing cyathanes diterpenes with good yields, and affords new cyathanes analogues including eriancines W, X, Y, ZA, ZB, and ZC. Our work also establishes an efficient platform for exploring the structural diversity in the family of cyathane-type diterpenes and elucidating the biosynthetic mechanisms of other cyathanes.

5. Experimental

5.1. *Strains and growth conditions*

H. erinaceus strain L547 was maintained on yeast malt medium (glucose 4.0 g/L, malt extract 10.0 g/L, yeast extract 4.0 g/L, and agar 20.0 g/L) plates at 28 °C for 7 days. *S. cerevisiae* BY-T20 and BJ5464-NpgA were grown on yeast extract peptone dextrose medium (YPD) plates at 30 °C. After transformation, *S. cerevisiae* strains were selected on synthetic dextrose complete medium (SDC) with appropriate supplements corresponding to the auxotrophic markers at 30 °C. For plasmids construction and amplification, *E. coli* strain DH5α was grown in liquid LB medium or solid medium (1.7% agar).

5.2. *RNA extraction and cDNA preparation*

The cultures of *H. erinaceus* in yeast malt medium were inoculated into yeast malt oat medium (glucose 4.0 g/L, malt extract 10.0 g/L, yeast extract 4.0 g/L, and oat 5.0 g/L). The fungal tissue was harvested. Total RNA was isolated using the TRIzol Reagent (Life Technologies) by using 60.0 mg of fungal sample. For degradation of genomic DNA and obtaining of cDNA, FastQuant RT Kit (TianGen Biotech) was used.

5.3. *DNA fragment construction, and plasmid construction*

PCR was performed using Phusion® High-Fidelity DNA Polymerase (NEB) or TransStart FastPfu DNA Polymerase (TransGen Biotech). The eri ORFs were amplified from cDNA of *H. erinaceus* L547. DNA fragments of *ncpr1* ORF, promoters, terminators, and homologous recombination regions of δ site and *rDNA* site were amplified from the genomic DNA of *S. cerevisiae* BY-T20. *AtUGD1* and *atUXS3* ORFs were amplified from the cDNA of *Arabidopsis thaliana* (gifted by Prof. Bo Yu). The assembly of DNA fragments was performed by using either Double-joint PCR strategy or Clone Express® MultiS One Step Cloning Kit (Vazyme Biotech)[52]. The primers were listed in Table S6. PCR products were confirmed by DNA sequencing. For expressing *eri* gene, each PCR product of *eri* ORFs was inserted into EcoRI/

NotI-digested pESC-TRP to give the plasmids listed in Supporting Information Table S7.

5.4. *Transformation of S. cerevisiae*

All of the transformants used in this work are listed in Table S1. For strains SC-G and SC-GI, the DNA fragments were integrated into the *δ* locus of BY-T20 *via* homologous recombination using S.c. EasyComp Transformation Kit (Invitrogen). Similarly, the linear DNA fragments were integrated into the *rDNA* locus of SC-GI to afford the following strains. The plasmids pESC-TRP-EriM, pESC-TRP-EriB, pESC-TRP-EriO, pESC-TRP-EriP were used for the transformation in BY-T20 to generate the strain SC-M, SC-B, SC-O and SC-P, respectively. The plasmids pESC-TRP-EriH was used for the transformation in SC-GICAJ to generate the strain SC-GICAHJ. For protein expression, the plasmids were introduced into *S. cerevisiae* BJ5464-NpgA to afford SC-Jp, SC-Hp, and SC-Pp.

5.5. *HPLC analysis of extracts*

Metabolites from the transformants, BY-T20, the *in vitro* reaction mixtures, and feeding experiments were analyzed by HPLC conducted on an Agilent 1290 HPLC System using an ODS column (C8, 250 mm × 9.4 mm, YMC Pak, 5 μm). The solvent system used was a gradient of 20%−40% acetonitrile/H_2O over 8 min, 40%−76% acetonitrile/H_2O over 27 min, 76%−100% acetonitrile/H_2O over 5 min, and 100% acetonitrile over 15 min with 0.01% trifluoroacetate at a flow rate of 1 mL/min.

5.6. *Non-enzymatic transformation of* ***3***

To determine the non-enzymatic transformation, erinacine P (**3**) was incubated in 100 μL buffer solution at 28 °C for 24 h. The pH value of the reaction mixture was regulated by 10 mmol/L Na_2HPO_4 and NaH_2PO_4. The mixture was analyzed by HPLC–MS eluted by a gradient of 20%−40% acetonitrile/H_2O over 8 min, 40%−76% acetonitrile/H_2O over 27 min, and 76%−100% acetonitrile/H_2O over 5 min with 0.05% formic acid at a flow rate of 1 mL/min. The mixtures were analyzed by HPLC.

5.7. *Neurotrophic activity*

The neuritogenic effects of compounds **12**−**14**, **19**, and **20** were examined according to an assay using PC12 cells as reported in the early research[34]. Assay was performed in 24-well plate with serum-free culture medium at a density of 4×10^4 cells/well. NGF was used as positive control. The percentage of cells showing neurite outgrowth was determined by light microscopy. Cells with neurites longer than or equal to twice the length of the diameter of the cell body were scored as positive. Neurite outgrowth was assayed from at least three different regions of interest in three independent experiments.

Acknowledgments

This work was supported by the grants from the National Key R&D program of China (Grant 2018YFD0400203 and 2017YEE0108200), the National Natural Science Foundation of China (Grant 21472233), and the "Innovative Cross Team" project, CAS (Grant E0222L01R1, China). We gratefully acknowledge Prof. Xueli Zhang (Tianjin Institute of Industrial Biotechnology, Chinese Academy of Sciences, China) for the kindly providing of yeast strains BY-T20. We thank Drs. Jinwei Ren and Wenzhao Wang (Institute of Microbiology, Chinese Academy of Sciences, China) for NMR and MS data collection.

Author contributions

Hongwei Liu and Ke Ma designed the research. Ke Ma and Yuting Zhang performed the experiments and analyzed the data under the guidance of Hongwei Liu, Bo Yu, and Wenbing Yin. Ke Ma and Yuting Zhang finished the sketch. Cui Guo, Yanlong Yang, Junjie Han, Bo Yu, and Wenbing Yin revised the manuscript. All authors contributed a lot to this work and approved the final version of the manuscript.

Conflicts of interest

The authors declare that there are no conflicts of interest.

Appendix A. Supporting information

Supporting information to this article can be found online at https://doi.org/10.1016/j.apsb.2021.04.014.

References

1. Hanson JR. Diterpenoids of terrestrial origin. *Nat Prod Rep* 2017;**34**:1233−43.
2. Ayer WA, Taube H. Metabolites of *Cyathus helenae.* A new class of diterpenoids. *Can J Chem* 1973;**51**:3842−54.
3. Tang HY, Yin X, Zhang CC, Jia Q, Gao JM. Structure diversity, synthesis, and biological activity of cyathane diterpenoids in higher fungi. *Curr Med Chem* 2015;**22**:2375−91.
4. Kawagishi H, Shimada A, Shirai R, Okamoto K, Ojima F, Sakamoto H, et al. Erinacines A, B and C, strong stimulators of nerve growth factor (NGF)-synthesis, from the mycelia of *Hericium erinaceum*. *Tetrahedron Lett* 1994;**35**:1569−72.
5. Friedman M. Chemistry, nutrition, and health-promoting properties of *Hericium erinaceus* (Lion's Mane) mushroom fruiting bodies and mycelia and their bioactive compounds. *J Agric Food Chem* 2015;**63**:7108−23.
6. Lee KF, Chen JH, Teng CC, Shen CH, Hsieh MC, Lu CC, et al. Protective effects of *Hericium erinaceus* mycelium and its isolated erinacine A against ischemia-injury-induced neuronal cell death *via* the inhibition of iNOS/p38 MAPK and nitrotyrosine. *Int J Mol Sci* 2014;**15**:15073−89.
7. Lee KF, Tung SY, Teng CC, Shen CH, Hsieh MC, Huang CY, et al. Post-treatment with erinacine A, a derived diterpenoid of *H. erinaceus*, attenuates neurotoxicity in MPTP model of Parkinson's disease. *Antioxidants* 2020;**9**:137.
8. Shimbo M, Kawagishi H, Yokogoshi H. Erinacine A increases catecholamine and nerve growth factor content in the central nervous system of rats. *Nutr Res* 2005;**25**:617−23.
9. Zhang CC, Cao CY, Kubo M, Harada K, Yan XT, Fukuyama Y, et al. Chemical constituents from *Hericium erinaceus* promote neuronal survival and potentiate neurite outgrowth *via* the TrkA/Erk1/2 pathway. *Int J Mol Sci* 2017;**18**:1659.
10. Enquist Jr JA, Stoltz BM. Synthetic efforts toward cyathane diterpenoid natural products. *Nat Prod Rep* 2009;**26**:661−80.

11. Wu GJ, Zhang YH, Tan DX, He L, Cao BC, He YP, et al. Synthetic studies on enantioselective total synthesis of cyathane diterpenoids: cyrneines A and B, glaucopine C, and (+)-allocyathin B_2. *J Org Chem* 2019;**84**:3223−38.
12. Wu GJ, Zhang YH, Tan DX, Han FS. Total synthesis of cyrneines A–B and glaucopine C. *Nat Commun* 2018;**9**:1−8.
13. Galanie S, Thodey K, Trenchard IJ, Interrante MF, Smolke CD. Complete biosynthesis of opioids in yeast. *Science* 2015;**349**:1095−100.
14. Ro DK, Paradise EM, Ouellet M, Fisher KJ, Newman KL, Ndungu JM, et al. Production of the antimalarial drug precursor artemisinic acid in engineered yeast. *Nature* 2006;**440**:940−3.
15. Wang WF, Xiao H, Zhong JJ. Biosynthesis of a ganoderic acid in *Saccharomyces cerevisiae* by expressing a cytochrome P450 gene from *Ganoderma lucidum*. *Biotechnol Bioeng* 2018;**115**:1842−54.
16. Yang YL, Zhang S, Ma K, Xu Y, Tao Q, Chen Y, et al. Discovery and characterization of a new family of diterpene cyclases in bacteria and fungi. *Angew Chem Int Ed* 2017;**129**:4827−30.
17. Liu C, Minami A, Ozaki T, Wu J, Kawagishi H, Maruyama JI, et al. Efficient reconstitution of Basidiomycota diterpene erinacine gene cluster in Ascomycota host *Aspergillus oryzae* based on genomic DNA sequences. *J Am Chem Soc* 2019;**141**:15519−23.
18. Kenmoku H, Sassa T, Kato N. Isolation of erinacine P, a new parental metabolite of cyathane-xylosides, from *Hericium erinaceum* and its biomimetic conversion into erinacines A and B. *Tetrahedron Lett* 2000;**41**:4389−93.
19. Bai R, Zhang CC, Yin X, Wei J, Gao JM. Striatoids A–F, cyathane diterpenoids with neurotrophic activity from cultures of the fungus *Cyathus striatus*. *J Nat Prod* 2015;**78**:783−8.
20. Kawagishi H, Shimada A, Hosokawa S, Mori H, Sakamoto H, Ishiguro Y, et al. Erinacines E, F, and G, stimulators of nerve growth factor (NGF)-synthesis, from the mycelia of *Hericium erinaceum*. *Tetrahedron Lett* 1996;**37**:7399−402.
21. Su P, Tong Y, Cheng Q, Hu Y, Zhang M, Yang J, et al. Functional characterization of *ent*-copalyl diphosphate synthase, kaurene synthase and kaurene oxidase in the *Salvia miltiorrhiza* gibberellin biosynthetic pathway. *Sci Rep* 2016;**6**:23057.
22. Kalb VF, Woods CW, Turi TG, Dey CR, Sutter TR, Loper JC. Primary structure of the P450 lanosterol demethylase gene from *Saccharomyces cerevisiae*. *DNA* 1987;**6**:529−37.
23. Oka T, Jigami Y. Reconstruction of *de novo* pathway for synthesis of UDP-glucuronic acid and UDP-xylose from intrinsic UDP-glucose in *Saccharomyces cerevisiae*. *FEBS J* 2006;**273**:2645−57.
24. Kenmoku H, Shimai T, Toyomasu T, Kato N, Sassa T. Erinacine Q, a new erinacine from *Hericium erinaceum*, and its biosynthetic route to erinacine C in the Basidiomycete. *Biosci Biotechnol Biochem* 2002;**66**:571−5.
25. Kenmoku H, Tanaka K, Okada K, Kato N, Sassa T. Erinacol (cyatha-3,12-dien-14β-ol) and 11-*O*-acetylcyathin A_3, new cyathane metabolites from an erinacine Q-producing *Hericium erinaceum*. *Biosci Biotechnol Biochem* 2004;**68**:1786−9.
26. Ayer WA, Browne LM. Terpenoid metabolites of mushrooms and related basidiomycetes. *Tetrahedron* 1981;**37**:2197−248.
27. Ayer WA, Yoshida T, van Schie DM. Metabolites of bird's nest fungi. Part 9. diterpenoid metabolites of *Cyathus africanus* Brodie. *Can J Chem* 1978;**56**:2113−20.
28. Zhang YT, Liu L, Bao L, Yang YL, Ma K, Liu HW. Three new cyathane diterpenes with neurotrophic activity from the liquid cultures of *Hericium erinaceus*. *J Antibiot* 2018;**71**:818−21.
29. Kasahara K, Miyamoto T, Fujimoto T, Oguri H, Tokiwano T, Oikawa H, et al. Solanapyrone synthase, a possible Diels–Alderase and iterative type I polyketide synthase encoded in a biosynthetic gene cluster from *Alternaria solani*. *ChemBioChem* 2010;**11**:1245−52.
30. Lambou K, Pennati A, Valsecchi I, Tada R, Sherman S, Sato H, et al. Pathway of glycine betaine biosynthesis in *Aspergillus fumigatus*. *Eukaryot Cell* 2013;**12**:853−63.
31. Hecht HJ, Höfle G, Steglich W. Striatin A, B, and C: novel diterpenoid antibiotics from *Cyathus striatus*; X-ray crystal structure of striatin A. *J Chem Soc Chem Commun* 1978;**15**:665−6.
32. Chen YR, Naresh A, Liang SY, Lin CH, Chein RJ, Lin HC. Discovery of a dual function cytochrome P450 that catalyzes enyne formation in cyclohexanoid terpenoid biosynthesis. *Angew Chem Int Ed* 2020;**59**:13537−41.
33. Shi XW, Liu L, Gao JM, Zhang AL. Cyathane diterpenes from Chinese mushroom *Sarcodon scabrosus* and their neurite outgrowth-promoting activity. *Eur J Med Chem* 2011;**46**:3112−7.
34. Marcotullio MC, Pagiotti R, Maltese F, Mwankie GN, Hoshino T, Obara Y, et al. Cyathane diterpenes from *Sarcodon cyrneus* and evaluation of their activities of neuritegenesis and nerve growth factor production. *Bioorg Med Chem* 2007;**15**:2878−82.
35. Joynera PM, Cichewicz RH. Bringing natural products into the fold-exploring the therapeutic lead potential of secondary metabolites for the treatment of protein-misfolding-related neurodegenerative diseases. *Nat Prod Rep* 2011;**28**:26−47.
36. Schobert R, Knauer S, Seibt S, Biersack B. Anticancer active illudins: recent developments of a potent alkylating compound class. *Curr Med Chem* 2011;**18**:790−807.
37. Zaidman BZ, Yassin M, Mahajna J, Wasser SP. Medicinal mushroom modulators of molecular targets as cancer therapeutics. *Appl Microbiol Biotechnol* 2005;**67**:453−68.
38. Chen HP, Liu JK. Secondary metabolites from higher fungi. In: Kinghorn AD, Falk H, Gibbons S, Kobayashi J, editors. *Progress in the chemistry of organic natural products 106*. Cham: Springer; 2017. p. 1−201.
39. Jacobsson S, Paukner S, Golparian D, Jensen JS, Unemo M. *In vitro* activity of the novel pleuromutilin lefamulin (BC-3781) and effect of efflux pump inactivation on multidrug-resistant and extensively drug-resistant *Neisseria gonorrhoeae*. *Antimicrob Agents Chemother* 2017;**61**:e01497.
40. Thomas JP, Arzoomanian R, Alberti D, Feierabend C, Binger K, Tutsch KD, et al. Phase I clinical and pharmacokinetic trial of irofulven. *Cancer Chemother Pharmacol* 2001;**48**:467−72.
41. Mori K, Inatomi S, Ouchi K, Azumi Y, Tuchida T. Improving effects of the mushroom Yamabushitake (*Hericium erinaceus*) on mild cognitive impairment: a double-blind placebo-controlled clinical trial *Phytother. Res* 2009;**23**:367−72.
42. Li I, Chang HH, Lin CH, Chen WP, Lu TH, Lee LY, et al. Prevention of early Alzheimer's disease by erinacine A-enriched *Hericium erinaceus* mycelia pilot double-blind placebo-controlled study. *Front Aging Neurosci* 2020;**12**:155.
43. Navale GR, Dharne MS, Shinde SS. Metabolic engineering and synthetic biology for isoprenoid production in *Escherichia coli* and *Saccharomyces cerevisiae*. *Appl Microbiol Biotechnol* 2021;**105**:457−75.
44. Caesar LK, Kelleher NL, Keller NP. In the fungus where it happens: history and future propelling *Aspergillus nidulans* as the archetype of natural products research. *Fungal Genet Biol* 2020;**144**:103477.
45. Oikawa H. Heterologous production of fungal natural products: reconstitution of biosynthetic gene clusters in model host *Aspergillus oryzae*. *Proc Jpn Acad Ser B Phys Biol Sci* 2020;**96**:420−30.
46. Paddon CJ, Westfall PJ, Pitera DJ, Benjamin K, Fisher K, McPhee D, et al. High-level semi-synthetic production of the potent antimalarial artemisinin. *Nature* 2013;**496**:528−32.
47. Srinivasan P, Smolke CD. Biosynthesis of medicinal tropane alkaloids in yeast. *Nature* 2020;**585**:614−9.
48. Liu T, Zhang C, Lu W. Heterologous production of levopimaric acid in *Saccharomyces cerevisiae*. *Microb Cell Factories* 2018;**17**:114.

49. Ignea C, Trikka FA, Nikolaidis AK, Georgantea P, Ioannou E, Loupassaki S, et al. Efficient diterpene production in yeast by engineering Erg20p into a geranylgeranyl diphosphate synthase. *Metab Eng* 2015;**27**:65−75.
50. Zhou YJ, Gao W, Rong QX, Jin GJ, Chu HY, Liu WJ, et al. Modular pathway engineering of diterpenoid synthases and the mevalonic acid pathway for miltiradiene production. *J Am Chem Soc* 2012;**134**: 3234−41.
51. Hu T, Zhou J, Tong Y, Su P, Li X, Liu Y, et al. Engineering chimeric diterpene synthases and isoprenoid biosynthetic pathways enables high-level production of miltiradiene in yeast. *Metab Eng* 2020;**60**: 87−96.
52. Yu JH, Hamari Z, Han KH, Seo JA, Reyes-Domínguez Y, Scazzocchio C. Double-joint PCR: a PCR-based molecular tool for gene manipulations in filamentous fungi. *Fungal Genet Boil* 2004;**41**: 973−81.